

EXPERIMENTAL AND THEORETICAL INVESTIGATION OF TENSILE STRESS DISTRIBUTION DURING ALUMINIUM WIRE DRAWING

O. M. Ikumapayi

S. J. Ojolo

S.A Afolalu

Department of Mechanical Engineering, University of Lagos, Lagos, Nigeria

Abstract

Wire drawing, has received a wide range of applications in the production. A wide number of cable applications demand that the cable survive high tensile loading. This work entails experimental and theoretical investigation of tensile stress distribution during aluminium wire drawing. The initial Aluminium rod used in this work was, 9.50mm with density of 2700kg/m^3 , young's modulus of ($7 \times 10^{10}\text{Pa}$), Poisson's ratio (0.33), Yield stress in simple tension ($21.7 \times 10^6\text{Pa}$), which was later drawn to different diameter as required and tensile testing was carried out on each required diameter.

In this work, tensile stress distribution in the drawing process is determined via experimental and analytical method. A free body equilibrium method is used to obtain the equations that dictate the drawing phenomenon. The result obtained by experiment is compared with improved model and also with other solutions found in the literature about these themes, particularly, with Rogas solutions in slab method case. There is high degree of similarity between the result obtained experimentally and the simulation of improved model but there is a wide gap when compared experimental result with simulation of classical slab method. Thus, the result of the study will be of great benefit to industries that make use of aluminium wire as electrical wiring, cables, spokes for wheels, stringed musical instruments, paper clips and tension-loaded structural components and also automotive sector. This will help them determining the extent of tensile loading that the aluminium wires their working on can withstand before failure can occur.

Keywords: Wire drawing; Classical Slab Method; Tensile Stress; Aluminium; Improved Method

Introduction

Aluminium wire is a type of wiring used in houses, power grids, and airplanes. Aluminium wires have been used mainly in overhead power lines and automobile battery cables, where the cross-section area of the conductor is large to support high current. Both tensile strength and electrical conductivity are required for automobile aluminium wires in which the former is the centre of discussion. Wires are used to bear mechanical loads and to carry electrical energy and/or communications signals. Wire has many uses. It forms the raw material of many important manufactures, such as the wire-net industry, wire-cloth making and wire-rope spinning, in which it occupies a place analogous to a textile fibre. Wire-cloth of all degrees of strength and fineness of mesh is used for sifting and screening machinery, for draining paper pulp, for window screens, and for many other purposes. Vast quantities of aluminium, copper, nickel and steel wire are employed for telephone and data wires and cables, and as conductors in electric power transmission, and heating. It is in no less demand for fencing, and much is consumed in the construction of suspension bridges, and cages, etc. In the manufacture of stringed musical instruments and scientific instruments wire is again largely used. Among its other sources of consumption it is sufficient to mention pin and hair-pin making, the needle and fish-hook industries, nail, peg and rivet making, and carding machinery; indeed there are few industries into which it does not enter.

Wiredrawing Process

Drawing process is one of the most used metal forming process within the industrial field and, particularly, in automotive and electric sectors. The process consists of reducing or changing the cross-section of pieces such as wires, rods, bars or plates, making pass them through a die by means of a pulling force (Rubio et al., 2005).

The wiredrawing is a plastic metal forming process, generally performed at cold working conditions, in which a suitably clean and lubricant coated wire is pulled through a die, which is a rigid tool with wear resistant surface. The longitudinal section of the die reduction region is shown in figure 1.

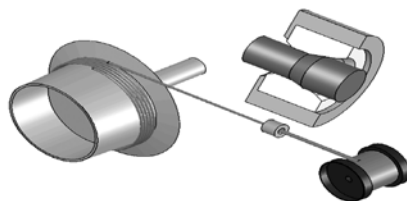


Fig 1: Scheme of the wiredrawing process.

This process is a complex interaction of many parameters (Kabayama and Taguchi, 2009) defined by:

1. Lubricant (friction coefficient, viscosity, surface treatment)
2. Wire properties (yield stress, elastic modulus, strain rate, strain hardening)
3. Die geometry (reduction angle, bearing region length, reduction area, and material).

The above mentioned parameters control the material deformation during the wire drawing process, and consequently, the stress distribution through the cross section of the drawn wire. With the correct parameter control, increased productivity and die life expectancy, as well as the wire breaking reduction will take place throughout the process. The parameter control also defines the wire properties such as good torsion resistance, tensile strength and rupture resistance (Shemanski, 1999).

The main variables involved in this drawing process comprise the die angle α , the cross-section A , the friction coefficient, μ , the area reduction r , and the yield tension, σ_x (see Fig. 2.1). It differs from other plastic forming processes primarily in that the traction tension applied to the working material is limited, and that the maximum tension allowed on the material section during drawing is equal to the yield tension.

The drawing process is characterised by two factors: a limit on the reduction that occurs during drawing; consumption of a fraction of the process potential by the frictional forces between the die wall and the material (Rogas 2008).

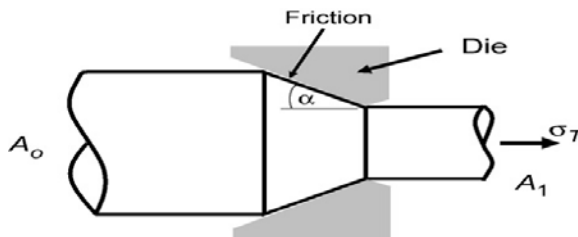


Fig. 2 – Axisymmetric die and wire (not to scale).

Several studies about wire drawing processes have been carried out. (Rogas et al., 2008) studied a new analytical solution for prediction of forward tension in the drawing process, in their studies results obtained from different simulations are reported, and validated against different analytical, numerical and experimental solutions. Specifically, the new solution (the third approximation of the yield criterion) is compared with the classical slab method (the first approximation), the second approximation, and the finite element method (FEM). Lastly, the model results are compared with experimental data reported by Wistreich (1958).

(Vega et al., 2009) have studied the effect of the process variables such as semi die angle and reduction in area, and the coefficient of friction on the drawing force value. Their results clearly indicate that friction has significant effects on the drawing force which decrease with the decrease of area reduction. The optimum die angle for wire drawing is assumed to be obtained when the plastic strain distribution across the diameter of the wire becomes uniform.

In recent past, some researchers had worked in similar field; (Leonardo et al, 2008) worked on the influence of die geometry on stress distribution by experimental and FEM simulation on electrolytic copper wire drawing. In their work, annealed electrolytic copper wire (ETP), with 0.5 mm original diameter was reduced by 19% in dies with $2\beta = 10^\circ$ and 18° and $H_c = 35$ and 50% . He then studied best his experimental results by the Finite Element Method to simulate residual stress distribution. The experimental results show that the friction coefficient decreases as the wire drawing speed increases, and that low 2β and H_c values bring about the most favourable wire drawing conditions. The simulation shows a variation in the axial and radial tensions, both for the compression and traction stresses on all regions during the wire drawing process. In conclusion, the influence of the internal die geometry on the drawn wire is clarified.

Cem, (2012), worked on the influences of some process parameters on cold working of ferrous wires. His experimental results shown that the tensile and torsion strength increase when reduction (deformation) ratio are increased. High reduction ratio causes maximum tensile strength and twist number (torsion strength) because of work (strain) hardening.

Another researcher, Rubio et al, (2005) worked on Calculation of the forward tension in drawing processes. Slab method and finite element method were being applied to calculate the drawing force necessary to carry out a wire and a plate drawing process. In their work, the main types of the drawing process has been analysed by means of the slab method and the finite element method. The obtained solutions have been tested with other ones found in the literature about this theme. Concretely, in the wire drawing case, with the experimental results given by (Wistreich, 1995) and, in the plate drawing case, with the empirical ones proposed by (Green and Hill, 1959) and with the obtained applying by the UBT. The solutions comparison confirms that FEM is a method more accurate than SM because they obtained results with it are nearer to the real results. FEM provides very intuitive simulations in which can be seen the forward tension not only at the die exit but in the deformation zone as well. However, FEM needs more calculation resources and good code knowledge by the users.

Materials, methods and model development

Material composition

A spark test analysis was carried out on the Aluminium sample to know its composition

Table 1: Aluminium Spectrometer analysis

Element	Al	Si	Fe	Cu	Mn	Mg	Zn	Ti	Cr
% Composition	99.58	0.14	0.23	0.0019	0.0065	0.0065	0.032	0.0075	0.0009

The aluminium rods were obtained as 9.50mm and were made ready to be tested. A test run was conducted to test the operating performance before conducting this actual test. Samples of the length required by standard which is 200mm (20cm) were cut from already drawn aluminium wire rod. Different diameters of sizes 1.70, 2.10, 2.50, 2.65, 3.10, 3.25, 3.40, 3.78, 4.00, and 4.40 all in mm were cut and measured with the aid of micrometer screw gauge.

Table 2 : Properties of the aluminium used in the process

Density, ρ	2700kg/m ³
Young's modulus, E	$7 \times 10^{10} Pa$
Poisson's ratio, ν	0.33
Yield stress in simple tension, Y	$21.7 \times 10^6 Pa$
Plane strain yield stress, S= 2K	1.155Y

Mathematical modelling of tensile stress distribution

Theoretical Background

A wire of initial diameter D_0 is drawn (pulled) through a conical portion of a die. While passing through the die, the wire deforms plastically and decreases in diameter. Frictional forces act between the wire metal and the rough die which aid the drawing process.

Model Development

Consider the drawing of wire as shown in figure 3, a slug of metal bonded by conical surface of the die and by two transverse surfaces normal to the axis of symmetry. One surface is at a distance x from the apex O of the die, and the other is at an additional incremental distance dx . The Stress σ_x over the transverse surface is assumed to be uniformly distributed tensile.

It is normal to the surface with no shear component. For the incremental distance dx the stress varies by the amount $d\sigma_x$. Over the

surface in contact with the conical die, a pressure, p is assumed normal to the surface and a friction drag T parallel to the surface.

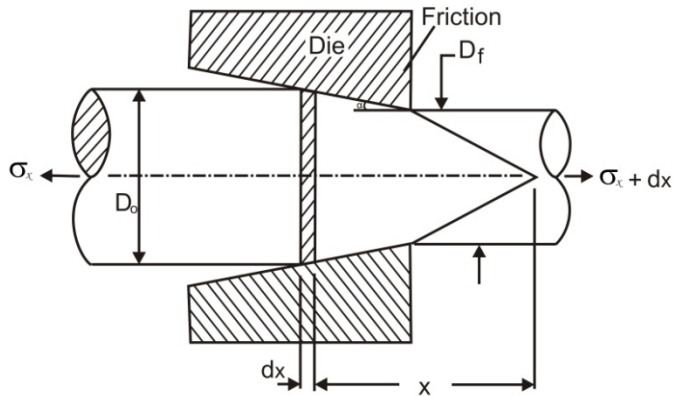


Fig. 3: Model of the plastically deforming zone for wire drawing

In obtaining the drawing process model, further assumptions are made

1. The friction at the die-material interface
- 1 obeys the Coulomb's law of sliding friction i.e the dynamic friction coefficient is constant
- 2 Cylindrical symmetry prevails
- 3 The die angle is small
- 4 The die is a rigid body and the drawing material is a rigid-plastic material
- 5 The average stresses is uniformly distributed within the element
- 6 The plastic deformation is Plane Strain.
- 7 The material flows into and out of the system horizontally i.e one-dimensional flow system prevails.

Equilibrium equations for symmetric and axisymmetric dies

To predict the drawing stress distribution, consider the free-body diagram of the material element shown in fig. 4.

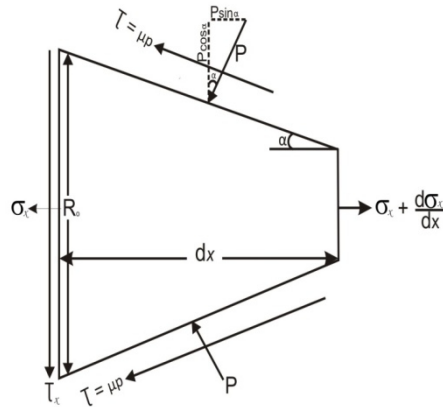


Fig. 4: Material element

(i) The component of the normal pressure of the die in the x-direction is

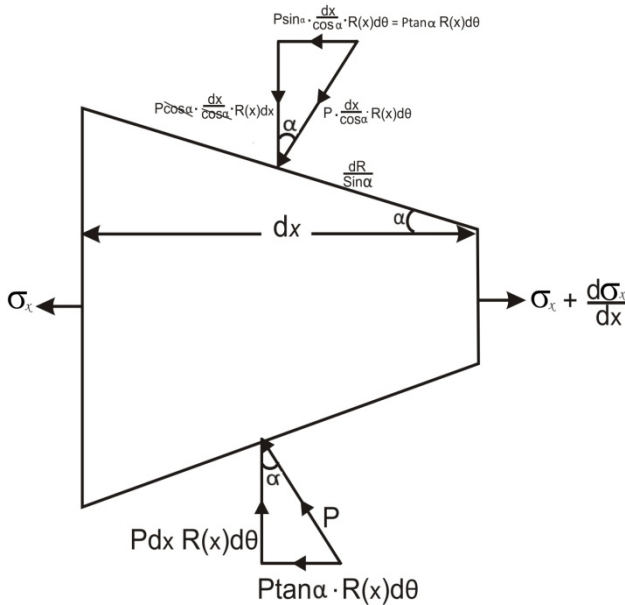


Fig.5: Stress state for infinitesimal triangular element

Projection of the Pressure forces on the die surface

$$\int_0^{2\pi} P \tan \alpha R(x) d\theta = P \pi R \tan \alpha = P \pi R dR \quad (1)$$

Where (α) = die angle

(ii) The component of the frictional stress τ in the x direction is

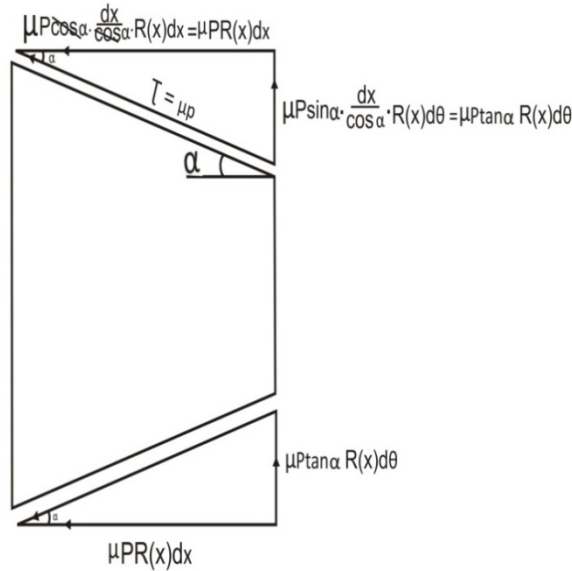


Fig. 6: Frictional stress for infinitesimal triangular element

Also, taking the integral of the frictional stress in the x direction

$$\int_0^{2\pi} \mu P dx R(x) d\theta = \frac{\mu P \pi R dx}{2} = \frac{\mu P \pi R dR}{2 \tan \alpha} \quad (2)$$

Balancing the forces, Equilibrium equation in the x direction will be

$$\left(\sigma_x + \frac{d\sigma_x}{dx} \right) \frac{\pi [R(x)]^2}{4} - \sigma_x \frac{\pi R_0^2}{4} - 2P \pi R(x) \frac{dR}{2} - 2 \frac{\mu P \pi R dR}{2 \tan \alpha} = 0 \quad (3)$$

Collect the like terms by multiplying through by $4 \tan \alpha$

$$\left[\sigma_x R^2(x) + \frac{d\sigma_x}{dx} R^2(x) - \sigma_x R_0^2 \right] \tan \alpha - 4P R(x) \tan \alpha dR - 4\mu P R(x) dR = 0 \quad (4)$$

In this equation above, the shear stress resulting from the frictional between the die and the material is considered to be equal to the product of the dynamic friction coefficient μ and the pressure p .

Dividing through by $R^2(x)$

$$\left[\sigma_x + \frac{d\sigma_x}{dx} - \sigma_x \left(\frac{R_0}{R_x} \right)^2 \right] \tan \alpha - \frac{4P}{R(x)} [\tan \alpha + \mu] dR = 0 \quad (5)$$

But

$$R(x) = R_0 - x \tan \alpha \Rightarrow \left(\frac{R_0}{R_x} \right)^2 = \left(1 + \frac{x \tan \alpha}{R(x)} \right)^2 \quad (i)$$

$$= \left(\frac{R_0}{R_x} \right)^2 = \left(1 - \frac{x dR}{R(x) dx} \right)^2 \quad (ii)$$

Substituting equation (ii) into equation (5)

Which gives

$$\frac{d\sigma_x}{dx} + \frac{n}{R(x)} \left[\sigma_x \frac{dR(x)}{dx} - P [\tan \alpha + \mu] \right] = 0 \quad (6)$$

Where the Constant n allows generalization of the equations for balancing forces

n = 1 for the problem of symmetric plane deformation

n = 2 for the problem of axisymmetric plane deformation

Using the dimensionless parameters X of position x

$$X = \frac{nxt \tan \alpha}{R_0 \left(\frac{A_0 - A_1}{A_0} \right)} \Rightarrow x = \frac{XR_0 \left(\frac{A_0 - A_1}{A_0} \right)}{n \tan \alpha} \text{ (iii)}$$

And

For conical dies, the contact zone between the die and the material has its slope defined by

$$\frac{dR}{dx} = -\tan \alpha$$

$$\frac{d\sigma_x}{dX} + \frac{\left(\frac{A_0 - A_1}{A_0} \right)}{\left(1 - \frac{x}{R_0} \tan \alpha \right) \tan \alpha} [-\sigma_x \tan \alpha - P[\tan \alpha + \mu]] = 0 \dots 7$$

Substituting equation (iii) into eqn (7)

$$\frac{d\sigma_x}{dX} + \frac{\left(\frac{A_0 - A_1}{A_0} \right)}{\left(1 - \frac{X \left(\frac{A_0 - A_1}{A_0} \right)}{n} \right) \tan \alpha} [-\sigma_x \tan \alpha - P[\tan \alpha + \mu]] = 0 \text{ (8)}$$

Let $\left(\frac{A_0 - A_1}{A_0} \right) = \beta$,

Then

$$\frac{d\sigma_x}{dX} - \frac{\beta}{\left(1 - \frac{\beta X}{n} \right) \tan \alpha} [\sigma_x \tan \alpha + P[\tan \alpha + \mu]] = 0 \dots 9$$

To solve equation (9), we need a function that relates the pressure P to the drawing Stress

CASE 1A: Assuming a linear relationship between P and σ_x

$$P = A - B\sigma_x$$

$$\frac{d\sigma_x}{dX} - \frac{\beta}{\left(1 - \frac{\beta X}{n} \right) \tan \alpha} [\sigma_x \tan \alpha + (A - B\sigma_x)[\tan \alpha + \mu]] = 0 \text{ (10)}$$

With the boundary condition X = 0, $\sigma_x = 0$

The above equation is of the form

$$\frac{dy}{dx} + P(x) = Q(x)$$

$$\sigma_x = \frac{A\beta(\tan \alpha + \mu)}{\tan \alpha} \left[1 - \left(1 - \frac{\beta}{n} X \right)^{\frac{n[\beta(1-B)\tan \alpha - \mu B]}{\beta \tan \alpha}} \right] \text{ (11)}$$

Therefore, equation (11) is the improved model

Case 1B:

Following Rogas *et al* (2008)

(1) Using the classical slab method

$$P = 2k - \sigma_x$$

Then $A = 2k, B = 1$

So,

$$\sigma_x = \frac{2k\beta(\tan\alpha + \mu)}{\tan\alpha} \left[1 - \left(1 - \frac{\beta}{n} X \right)^{\frac{n \mu}{\beta \tan\alpha}} \right] \dots 12$$

Therefore, equation 11 and 12 are improved model and classic slab method model respectively.

Results and discussion

Table 3 shows the experimental results obtained from the tensile stress test for different sizes for unstranded wire drawing. The initial diameter of the wire rod was 9.50mm (9.50x10⁻³m). The tensile strength was conducted for the unstranded wire drawing to determine the variation in the tensile strength.

Table 3: Tensile Strength values for un-stranded wire drawing

$$D_0 = 9.50\text{mm} = 9.50 \times 10^{-3}\text{m},$$

$$\beta = 8^\circ, \quad 2\alpha = 12^\circ, \quad \alpha = 6^\circ$$

S/N	D _i (mm)	F _m (N)	A (m ²) 10 ⁻⁶	$\sigma = \frac{F}{A} \left(\frac{N}{m^2} \right)$	$1 - \frac{D_i^2}{D_0^2}$
1	1.70	427.90	2.27	188.50	0.9680
2	2.10	626.50	3.46	181.07	0.9511
3	2.50	864.10	4.91	176.11	0.9310
4	2.65	959.50	5.52	173.82	0.9222
5	3.10	1258.80	7.55	166.73	0.8940
6	3.25	1370.90	8.30	165.17	0.8830
7	3.40	1496.00	9.08	164.00	0.8720
8	3.78	1820.00	11.22	162.20	0.8417
9	4.00	2030.00	12.57	161.50	0.8227
10	4.40	2433.60	15.21	160.00	0.7855

Table 3 show the Tensile strength values for unstranded wire drawing. It was observed that the tensile stress decreases as diameters increase in size. At the same time, as the diameter increases the breaking load (force) requires deforming it also increases. It is also evidence in the table that, decrease in stress also lead to decrease in reduction area i.e the higher the reduction area, the higher the stress.

The effect of tensile strength on reduction ratio of the experimental result is as shown in **fig 7**; the graph reveals that increase in reduction ratio (deformation) leads to increase in tensile strength and vice-versa. The tensile strength is slightly directly proportional to reduction (deformation) ratio. This was as proposed by Cem (2012) and Narayanan, et al. (2010). High reduction ratio causes maximum tensile strength. It is also evidence from the graph that there is sporadic increase in tensile strength from 166.73 to 188.50MPa when the reduction ratios increase from 0.8940 to 0.9680.

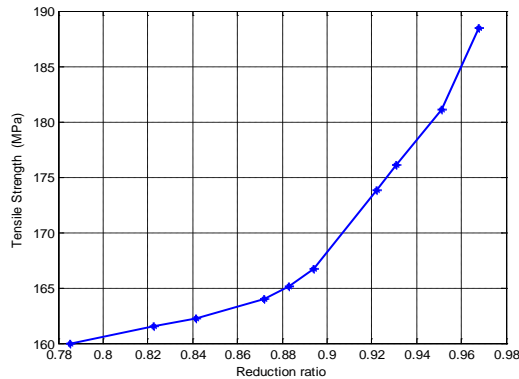


Fig 7: Effect of tensile strength on reduction ratio

Fig 8, shows the dimensionless drawing tension, for symmetric geometry ($n=1$), a reduction r of 0.2, and a friction coefficient μ equal to 0.15. Compare with the **fig 9** where the coefficient of friction is 0.10 with the maximum tensile stress of 11MPa, 0.11 with the maximum tensile stress of 12.2MPa, 0.12 with the maximum tensile stress of 13.8MPa, and in this fig4.4 , where the coefficient of friction has increased to 0.15, leads to maximum tensile stress of 17.0MPa. It therefore shows that slight increase in friction coefficient will invariably increase the tensile stress during aluminium wire drawing. This also was in agreement of the report of Rubio et al. (2005) when comparing the FEM solution with Slab method.

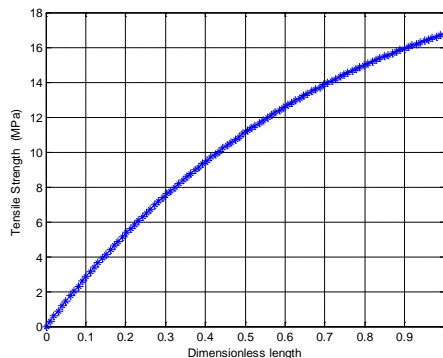


Fig 8: Dimensionless drawing tension for symmetric plane deformation

Fig 9 shows the effect of tensile strength on dimensionless length for symmetric plane deformation at different Coefficient of friction, for symmetric geometry ($n=1$), a reduction r of 0.2, and a friction coefficient μ equal to 0.10, 0.11 and 0.12. The graph reveals that increase in friction for symmetric plane deformation leads to increase tensile stress of the material. i.e the higher the friction during drawing the higher the tensile stress of the material. It is evidence from the graph that where the coefficient of friction is 0.10 the maximum tensile stress is 11MPa, 0.11 the maximum tensile stress is 12.2MPa, and 0.12 the maximum tensile stress is 13.8MPa.

This can be further explain that during wire drawing, friction must be reduced to minimum because the more the fiction generated during wire drawing the more the induced tensile stress, this was confirmed by the report of Rogas et al. (2008) using finite element method (FEM) and work proposed by (Rubio et al., 2005) when comparing FEM result with Slab methods of Coulomb friction value equal to 0.10 and 0.20.

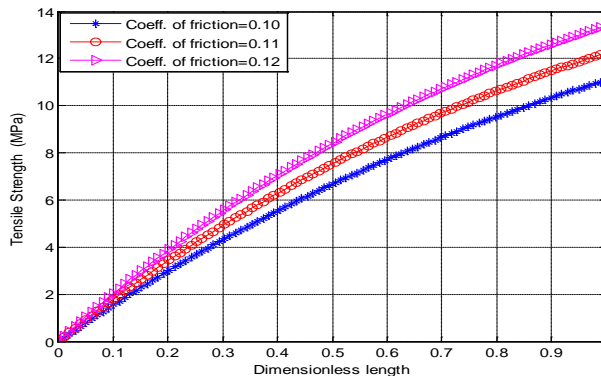


Fig 9: Effect of tensile strength on dimensionless length for symmetric plane Deformation at different coefficient of friction

Comparison of the Experimental result and the simulation of slab method is as shown in the **fig 10**. From the graph, one can infer that experimental result and simulated classical slab method are not so close but they all seem to take the same pattern. Both Experimental and simulated classical slab method took the same pattern. Both predict that the higher the reduction ratio the higher the tensile stress; and the lower the reduction ratio, the lower the tensile stress of the material. The graph also shows that there is a wide margin in terms of prediction when compare experimental result with classical slab model. This was also supported when compare the Finite element method, Slab method by Rubio et al. (2005). In their report FEM and Wistreich's experimental solutions are bigger than SM ones.

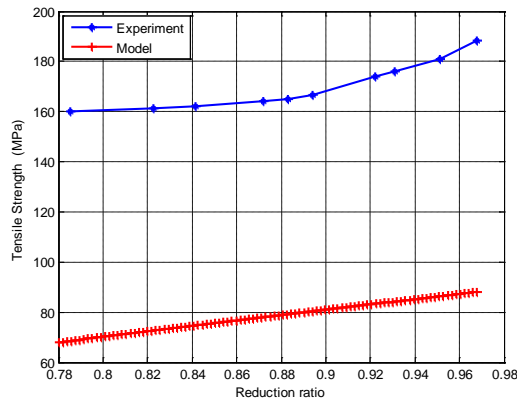


Fig 10: Comparison of the Experimental result and the simulation of slab method

Fig.11 shows the comparison of the effect of half conical angle on the tensile strength for symmetric and axisymmetric plane deformation. From the graph, for both symmetric and axisymmetric, as the half conical angle reduces to minimum, the tensile stress increases to the highest. It can be seen from the graph that, the optimal semi conical angle is 6°. At this point, the symmetric and axisymmetric begins to part against 8° used during the experiment. Semi conical angle must not be too small and must not be too large. It must be moderate for both symmetric and axisymmetric plane deformation. This prediction was also in agreement with the proposed work of Rogas et al. (2008) and the work of (Rubio et al., 2005). Minimum drawing tension generally occurs between 3.5° and 14° (Avitzur, 1997). Also Rubio et al. (2005) found that the minimum drawing tension lies within the range of 8° – 14°. The former can be thus used to determine the die angle which minimizes the drawing tension, as the prediction in said range is good as against the one found in this report which ranges from 8° to 18°.

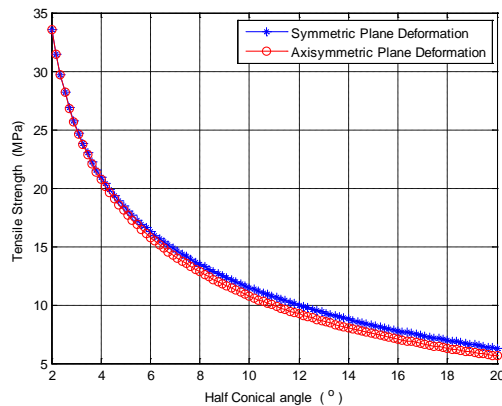


Fig 11: Comparison of the effect of Half Conical angle on the tensile strength for Symmetric and axisymmetric plane deformation

Fig 12 reveals the comparison of the effect of Half Conical angle on tensile strength at coefficient of friction of 0.1 and 0.2. The graph reveals that coefficient of friction play important role in tensile strength distribution during wire drawing as well as semi conical angle. The graph shows that increase in friction coulomb increases the tensile strength of aluminium during wire drawing. Similarly, decrease in semi conical angle will increase the tensile stress distribution during wire drawing. One can infer from the graph that coulomb friction is directly proportional to tensile strength while semi conical angle is inversely proportional to tensile strength. This was as reported by Rubio et al. (2005) and Rogas et al. (2008).

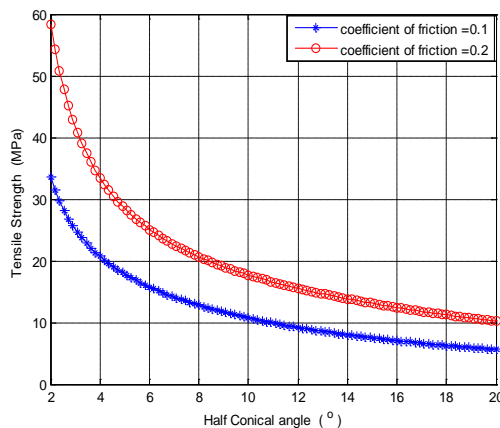


Fig 12: Comparison of the effect of Half Conical angle on tensile strength at coefficient of friction of 0.1 and 0.2

Fig 13 reveals the comparison of experimental result with simulated model results. In the graph, experimental result is being compared with model classical slab method and improved model result. The graph reveals that, the experimental curve and simulated improved model are very close, they both follow the same trend. While model of classical slab method is far away from them. This validates the experiment to predict tensile stress distribution during aluminium wire drawing as both the experiment and improved model agreed. The experiment and simulated improved model are much closer than simulated classical slab method. Thus, the prediction with improved model is better than that made by classical slab method when compare with the experimental result. The experimental result, improved model and classical slab method was in agreement with the report made by Rubio et al. (2005), Rogas et al. (2008) and the experimental result of Wistreich. As the experimental result and improved model results are much closer in my research work, so also the FEM of Rubio and Wistreich experiment are much closer but far away from the Slab method solution as predicted.

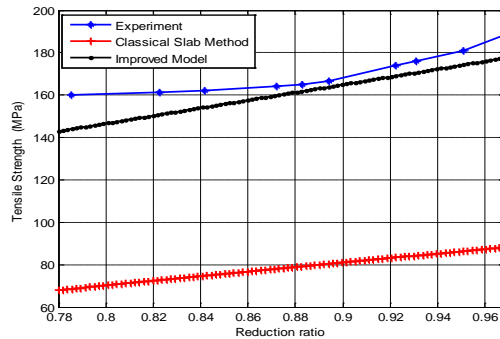


Fig 13: Comparison of Experimental Result with Model Simulation Results

Conclusion

Drawing process has been studied by means of different methods in recent years as a result of its great important in the industrial sector. In this work, the tensile strength distribution during aluminium wire drawing has been studied experimentally and theoretically. The result obtained was validated by the improved model and classical slab method. From the results obtained and their discussions, the following conclusions were drawn from the research carried out

Tensile Strength increases with decrease in the ratio of final diameter to initial diameter

The experiment and models have shown that the tensile strength increase when reduction (deformation) ratio are increased and vice-versa. High reduction ratio causes maximum tensile strength; this also was as predicted by Cem (2012) and Narayanan, et al. (2010).

The higher the diameter, the higher the breaking load (Force) needed to fracture it and vice-versa

Increase in frictional coulomb increases the tensile strength during drawing

For both symmetric and axisymmetric plane deformation, reduction in half conical angle will lead to increase in tensile strength. It was also revealed that half conical angle must not be too small or too large for optimal production.

References:

- Aernoudt E. (1989): "Materials response to wiredrawing", *Wire Journal International*, 22(3): 53-75.
- Alexander, J. M. (1965): "Hydrostatic Extrusion of Wires," *Journal of the Institute of Metals*, Vol. 93, pp. 366–369.

- Andrus, P., and Schmehl, G. (1976): “Continuous Hydrostatic Wire Extrusion,” Paper No. MF76-409, p. 16, Society of Manufacturing Engineers, Dearborn, Michigan
- Avitzur, B. (1997): Limit analysis of flow through conical converging dies, in: Proceedings of the JSTP International Seminar of Precision Forging, Osaka, Japan, Paper.
- Avitzur B. (1983): ”*Handbook of Metal Forming*”, New York, EUA: John Wiley and Sons
- Bridgman, P. W. (1952):”*Studies in Large Plastic Flow and Fracture*”, McGraw-Hill Book Company.
- Budinski, K.G., and Budinski, M.K. (2004): “Engineering Materials: Properties and Selection” 8th ed, Prentice Hall, .). Upper Saddle River, NJ: Prentice-Hall, Inc. ISBN 0-13-367715-X
- Caddell, R. M., and Atkins, A. G. (1968): “The Influence of Redundant Work When Drawing Rods through Conical Dies,” *Journal of Engineering for Industry*, Vol. 90, pp. 411–419
- Camacho, A.M., Domingo, R., Rubio, E.M., and González, C. (2005):“Analysis of the influence of back-pull on drawing process by the Finite Element Method”, *Journal of Materials Processing Technology*. 164-165; 1167-1174.
- Cem, S. C., (2012): ”A study on influence of some process parameters on cold drawing of ferrous wires”, department of Mechanical Engineering, Faculty of Engineering and Architecture, Trakya University, 22180 Edime, Turkey
- Degarmo, E. P., Black, J .T., Kohser, R. A. (2003): “*Materials and Processes in Manufacturing*”, (9th ed.), Wiley, [ISBN 0-471-65653-4](#)
- Dixit, P.M., and Dixit, U.S. (2008): Modeling of Meta Forming and Machining Processes by Finite Element and Soft Computing Methods. pp 12, Engineering Materials and Processes ISSN 1619 – 0181. Published by Springer-Verlag London Limited, British Library Cataloguing in Publication Data, Library of Congress Control Number: 2008926767.
- Dixon, R. F. (1987):“Company Works to Develop Die-Less Drawing Process,” *Wire Journal International*, Vol. 20, No. 10, pp. 25–26 and 28, The Wire Association International, Inc., Guilford, Connecticut
- Doege, E. K. A., and Massai, A.M. (2000): “Stress and strain analysis of automated multistage FEM-simulation of wiredrawing considering the backward force”, *Wire Journal International*, 33(5):144-149.
- Flanders, N. A., and Alexander, E. M. (1979): “Analysis of Wire Temperature and Power Requirements on Multi-Pass Drawing Productivity,” The Wire Association International, Inc
- Fowler, T., and Lancaster,P. R. (1983): “Factors Limiting Speed in Wire Drawing,” *Wire Industry*, Vol. 50, No. 592, pp. 208-211

- Hosford, W.F., Caddell, R.M., (1993):”Metal Forming Mechanics and Metallurgy”. Prentice-Hall, Englewood Cliffs, NJ.
- Hunter, C. (2006): “Aluminum Building Wire Installation and Terminations”
- Kabayama, L.K., and Taguchi, S.P. (2009):”The influence of Die Geometry on stress Distribution by Experimental and FEM Simulation on Electrolytic copper wiredrawing”. Department of materials Engineering – DEMAR, Engineering School of Lorena _ EEL. *Journal of materials Research*, Vol 12, no 13, pp 281 – 285
- Khateeb, M. H., and Donna H. (1994):”Repairing Aluminum Wiring”, Consumer Product Safety Commission, Telecommunications and networks,
- McClellan, G. D. S. (1952): “Some Friction Effects in Wire Drawing,” *Journal of the Institute of Metals*, Vol. 81, pp. 1–13
- Milenin, A. and Kustra, P. (2013): “Numerical and Experimental analysis of wire drawing for hardly deformable biocompatible magnesium alloys”. *Archives of metallurgy and materials*, vol 58, issue 1, pp 59
- Nakagari ,A., Yamano ,T., Konaka, M., Asakawa, M., Sasaki, W., and Yoshida, K.(1999):”Behavior of Residual stress and drawing stress in conical-type die and circle-type die drawing by the FEM simulation and experiment” *Proceedings of The Wire Association International Conference, Inc. Wire & Cable Technical Symposium (WCTC), 69th Annual Convention*; Atlanta, Geórgia, USA
- Narayanan, K.R., Sridhar, I., Subbiah, S. (2010):”Effect of cold work on the mechanical response of drawn ultra-fine gold wire”. *Computational materials science*, 49 (1), S119 – S125
- Ranger, A. E. (1957): “An Electrical Analogue for Estimating Die Temperatures during Wire Drawing,” *Journal of the Iron and Steel Institute*, Vol. 185, pp. 383–388
- Renz, P., Steuff, W., and Kopp, R. (1996):”Possibilities of influencing residual stresses in drawn wires and bars”, *Wire Journal International*, 29(1):64-69
- Rogas, G.H.A., Calvet, J.V.,Bubnovich, V.I. (2008): Anew analytical solution forprediction of forward tension in the drawing process. *Journal of Materials Processing Technology* Page 93 – 98
- Rubio, E.M., Camacho, A.M., Sevilha, L., and Sebastián, M.A.(2005):“Calculation of the forward tension in drawing processes”, *Journal of Materials Processing Technology*; 162-163 (2005) 551-557.
- Shemenski, R.M. (1999):”Wiredrawing by computer simulation”, *Wire Journal International*, 32(4):166-183.
- Wistreich, J. G. (1958): “The Fundamentals of Wire Drawing,” *Metallurgical Reviews*, Vol. 3, No. 10, pp. 97–141